ELSEVIER

Contents lists available at ScienceDirect

## Science of the Total Environment

journal homepage: www.elsevier.com/locate/scitotenv





## Coastal eutrophication driven by long-distance transport of large river nutrient loads, the case of Xiangshan Bay, China

Xiangyu Sun<sup>a,b</sup>, Jingjing Zhang<sup>b,c,d</sup>, Hongliang Li<sup>b,c,d,\*</sup>, Yong Zhu<sup>b</sup>, Xingju He<sup>b</sup>, Yibo Liao<sup>b</sup>, Zhibing Jiang<sup>b</sup>, Lu Shou<sup>b</sup>, Zhiwen Wang<sup>e</sup>, Tim C. Jennerjahn<sup>f,g</sup>, Jianfang Chen<sup>b,h</sup>

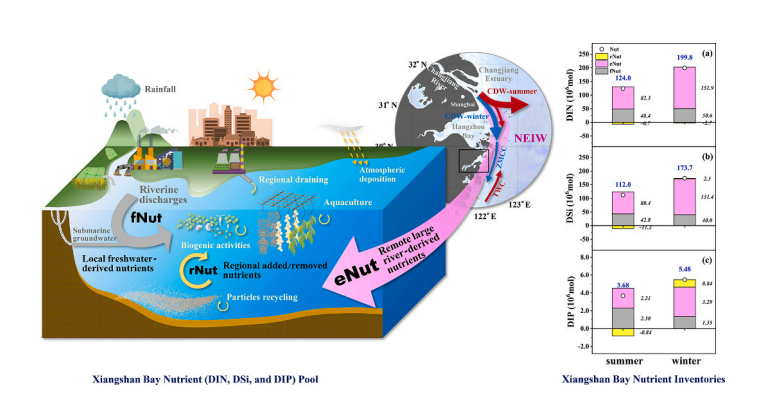
- <sup>a</sup> Ocean College, Zhejiang University, Zhoushan 316021, China
- b Key Laboratory of Marine Ecosystem Dynamics, Second Institute of Oceanography, Ministry of Natural Resources, Hangzhou 310012, China
- <sup>c</sup> Southern Marine Science and Engineering Guangdong Laboratory (Zhuhai), Zhuhai 519082, China
- d Observation and Research Station of Yangtze River Delta Marine Ecosystems, Ministry of Natural Resources, Zhoushan 316021, China
- <sup>e</sup> Key Laboratory of Ocean Space Resource Management Technology, MNR, Marine Academy of Zhejiang Province, Hangzhou 310012, China
- f Leibniz Centre for Tropical Marine Research, D-28359 Bremen, Germany
- <sup>8</sup> Faculty of Geoscience, University of Bremen, D-28359 Bremen, Germany
- <sup>h</sup> State Key Laboratory of Satellite Ocean Environment Dynamics, Hangzhou 310012, China

## HIGHLIGHTS

## Eutrophication in Xiangshan Bay is driven by distant Changjiang River nutrient load.

- Contributions of the outer bay-derived DIN and DSi were more significant than DIP.
- Inter-regional management is recommended for coastal bay eutrophication mitigation.

#### G R A P H I C A L A B S T R A C T



## ARTICLE INFO

Editor: Jay Gan

Keywords:
Coastal eutrophication mitigation
Nutrient source
Changjiang diluted water
Xiangshan Bay

## ABSTRACT

With accelerating anthropogenic activities, the overloading of land-derived nutrients and the resultant eutrophication are threatening coastal aquatic habitats worldwide. In semi-enclosed coastal bays, eutrophication is always considered a local problem that can be mitigated by nutrient reduction at a regional scale. However, as the main nutrient drains major global river discharges can have far-reaching effects over hundreds of kilometers alongshore, which are usually not precisely recognized in local coastal zone management. Here, we first quantified the contributions from both local and remote nutrient sources in Xiangshan Bay (XSB), a eutrophic semienclosed bay in China 200 km south of the mouth of the Changjiang River (CJR, the world's third largest river), employing a salinity-based conservative mixing model. We found that the nutrients in Xiangshan Bay were mainly supplied by intruded coastal water fed by CJR discharge, contributing 63 % of dissolved inorganic

E-mail address: lihongliang@sio.org.cn (H. Li).

<sup>\*</sup> Corresponding author at: Key Laboratory of Marine Ecosystem Dynamics, Second Institute of Oceanography, Ministry of Natural Resources, Hangzhou 310012, China.

nitrogen (DIN), 65 % of dissolved silicon (DSi), and 49 % of dissolved inorganic phosphorus (DIP) during the summer of 2017, and 75 % of DIN, 75 % of DSi and 60 % of DIP during the winter of 2019. Additionally, long-term interannual trends in the nutrient concentrations of XSB were generally synchronous with those of the downstream portion of the CJR, indicating that CJR discharge seems to be a strong driver of the eutrophication observed in XSB. In contrast, the impact of local nutrient inputs, such as riverine sewage drainage, aquaculture, biogenic activities, and elemental recycling, was much lower and was regionally limited to the inner bay. Interestingly, the DIP contributions of the local and remote sources were similar, indicating the greater relevance of the internal process. Overall, to mitigate eutrophication in large river-adjacent coastal bays, the inter-regional united practices for nutrient source regulation and ecosystem restoration should be permanently applied along the entire river basin-estuary-coastal continuum.

#### 1. Introduction

Eutrophication in coastal marine ecosystems is generally caused by nutrient overloading and has become severe in recent decades, owing to the impact of accelerating anthropogenic activities (Conley et al., 2009; Nixon, 1995). Fertilizer use, fossil fuel emissions, and industrial wastewater release significantly increase the nitrogen (N) and phosphorous (P) concentrations in coastal waters (Conley et al., 2009; Galloway et al., 2008). As the controlling nutrient for diatom growth, coastal silica (Si) is affected by complex factors, including increased weathering triggered by global warming and decreased export due to the construction of dams and reservoirs along river basins, leading to a change in N:P:Si ratios (Gaillardet et al., 1999; Humborg et al., 1997; Nixon, 1995). Consequently, a series of ecosystem problems ensue, such as the proliferation of harmful algal blooms (HAB), oxygen deficiency or even hypoxia/ anoxia, food web structure disruption, and habitat loss of living organisms (Anderson et al., 2002; Hallegraeff, 1993; Schindler, 2006). Thus, the identification of nutrient sources, source contributions, and proper strategies for nutrient management are urgently required for the sustainability of coastal water ecosystems and human living conditions.

Coastal bays usually suffer from serious eutrophication because of their semi-enclosed nature, complex hydrodynamics, dense populations, and various nutrient sources (Cloern et al., 2020; Greening et al., 2014; Han et al., 2021; Lane et al., 2010; Murphy et al., 2022). Local anthropogenic activities that include nutrient inputs are generally regarded as the main cause and have led to sustained efforts for decades to facilitate emission reduction of local wastewater and agricultural release (Boesch, 2019). These management measures have been proven to effectively mitigate eutrophication in estuarine bays such as Tampa Bay and Chesapeake Bay, USA (Greening et al., 2014; Murphy et al., 2022). In the case of bays with intensive aquaculture activities such as Sanggou Bay, China, ameliorative integrated multi-trophic aquaculture has also helped reduce nutrients and recover the inner-bay ecosystem (Fang et al., 2016). However, such local nutrient reduction strategies are rarely successful in other types of bays, such as those near large river estuaries.

Large rivers are the major drains of land-derived substances, especially nutrients (Seitzinger et al., 2005), which may extend along the coast over hundreds of kilometers driven by wind and tides (Horner-Devine et al., 2015), and possibly reach the mouth of adjacent, or even distant bays (Wu et al., 2019; Yang et al., 2018). For bays without strong local flushing, the inner-bay water is mainly supplied by externally intruded coastal water (Bugica et al., 2020; Lao et al., 2022a), which is usually considered to dilute the local land-derived nutrient load accumulated in a semi-enclosed bay with a long residence time (Duarte and Krause-Jensen, 2018). Nutrient enrichment and eutrophication are continually reported in the world's major river estuaries, adjacent coastal waters, and connected open gulfs, such as in the northern Gulf of Mexico which is mainly fed by the Mississippi and Atchafalaya Rivers, and in Chinese coastal waters fed by three major rivers, the Changjiang River, Pearl River, and Yellow River (Boesch, 2019; Lao et al., 2023; Strokal et al., 2014; Turner et al., 2012). The supply of remote nutrient sources, i.e. long distance transportation of the coastal currents fed by large river-derived nutrients, is noticed at the mouth of the coastal bays (Han et al., 2021; Lane et al., 2010; Lao et al., 2022a; Lao et al., 2022b;

Yang et al., 2018), and the coastal bays adjacent to the large river estuary are always seems to be more eutrophic than the bays without the impact of a large river discharge (e.g., Hangzhou Bay adjacent to Changjiang estuary and Fourleague Bay adjacent to the Atchafalaya River) (Lane et al., 2010; Wang et al., 2021b; Wu et al., 2019). However, much less is known about the quantitative contribution of such nutrient-laden water masses on the entire environmental conditions of the semienclosed coastal bays, which are often the resource base of the local population.

The Changjiang River (CJR, or Yangtze River) is one of the world's largest rivers, delivering  $115 \pm 6.26 \times 10^9$  mol yr<sup>-1</sup> of dissolved inorganic nitrogen (DIN), 96.7  $\pm$  5.6  $\times$   $10^{9}$  mol yr  $^{-1}$  of dissolved silicon (DSi), and 1.79  $\pm$  0.13  $\times$  10<sup>9</sup> mol yr<sup>-1</sup> of dissolved inorganic phosphorus (DIP) into the East China Sea (ECS) and Yellow Sea during the mid-2000s to the mid-2010s, which increased dramatically since the 1980s due to accelerating fertilization and urbanization along the river basin (Liu et al., 2018; Zhang et al., 2021). Driven by the Asian monsoon, the tides, and discharge variation, the majority of the CJR plume extends southward along the coast of the Zhejiang and Fujian provinces in winter, possibly reaching the Taiwan Strait about 600 km away, which is known as the Zhe-Min Coastal Current (ZMCC) (Wu et al., 2021; Zhang et al., 2022); while in summer, the southward alongshore transportation of the Changjiang Diluted Water (CDW) is relatively weak, with the major plume extending north-eastward offshore (Beardsley et al., 1985; Wu et al., 2014). The mean annual runoff of downstream CJR was  $8931 \times 10^9 \text{ m}^3 \text{ yr}^{-1}$  according to Changjiang Water Resources Commission, China (http://www.cjh.com.cn/), which was much larger than that of the Qiangtangjiang River ( $166 \times 10^9 \text{ m}^3$ yr<sup>-1</sup>) (Zhang et al., 2015), the largest local river discharge in Zhejiang Province. Considering the great disparity of the runoff between CJR and the other local river discharges alongshore, the nutrient-laden CDW is undoubtedly the main source of freshwater and nutrients for the northern ECS inshore water (NEIW) (Fig. 1a).

Xiangshan Bay (XSB), a semi-enclosed bay about 200 km south of the CJR mouth, is one of the most eutrophic bays along the Chinese coast (Fang et al., 2021). Large-celled phytoplankton (mostly diatoms and harmful dinoflagellates) blooms frequently occur in this temperate bay with sufficient nutrient supply, relatively stable water flow, and increasing temperature (Jiang et al., 2019b), resulting in food web simplification and ecosystem degradation (Du et al., 2020). Aquaculture effluents and land-derived nutrient loads, including local river catchment, sewage draining, and agricultural wastewater release are the major local nutrient sources (Nobre et al., 2010). However, management interventions to reduce the locally-derived inputs since the mid-2000s did not efficiently reduce the nutrient inventories of the whole inner bay, which were to restrict land input, such as fertilizers use, and to decrease the overloading of nutrients during the aquaculture activities (Ning and Hu, 2002; Wu et al., 2013; Yang et al., 2018), indicating that it is fueled by another source. Therefore, we hypothesized that this is a remote effect of the nutrient-laden CJR plume. The objectives of this study were to (1) quantify the nutrient fluxes introduced by the remote alongshore-transported large river discharge, local draining, and internal recycling in XSB; (2) evaluate the far-reaching effect of CJR discharge on XSB on seasonal and interannual scales; and (3) provide

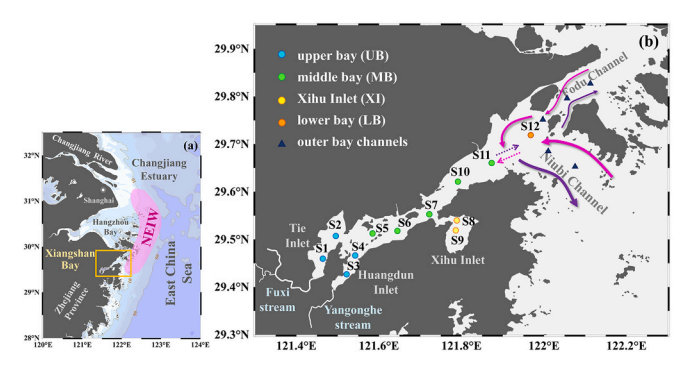


**Fig. 1.** The maps of the study area. The location of Xiangshan Bay and the northern ECS inshore water (NEIW) are shown in Figure (a) by yellow box and pink shading. Study sites during the 2017 summer and 2019 winter cruises are shown in Figure (b) by dots, with the four segments, i.e. upper bay (UB), middle bay (MB), Xihu Inlet (XI), and lower bay (LB) distinguished by blue, green, yellow, and orange, respectively. The hydrological study sites of outer bay channels are shown by dark blue triangles. The horizontal tidal residual circulation in the outer bay channels is shown by the pink (intrusion) and purple (export) solid arrows, and the inner bay circulation is shown by the dotted arrows, with the bottom water intruding and surface water exporting.

suggestions for nutrient reduction in eutrophic coastal bays under a systemic view of the land-ocean aquatic continuum.

## 2. Materials and methods

#### 2.1. Study area

Xiangshan Bay (XSB) is a narrow and shallow bay, with a length of about 60 km (Fan and Jin, 1989). The bay covers an area of 560 km<sup>2</sup>, including approximately 30 % tidal flats and 70 % permanently watercovered areas (Ning and Hu, 2002). Three branching bays, Tie Inlet (TI), Huangdun Inlet (HI), and Xihu Inlet (XI) open into the upper and middle bay. Surrounded by low hills and small rivers, the local freshwater discharges into XSB are very limited (the total mean annual runoff of all the river discharges to XSB is  $1.29 \times 10^9$  m<sup>3</sup> yr<sup>-1</sup>, which is about 0.15 % of the CJR annual runoff), with two of the major local rivers, Fuxi Stream and Yangonghe Stream, draining into upper branching bays (Gao et al., 1990; Yuan et al., 2014). Driven by horizontal tidal residual circulation, the adjacent NEIW constantly intrudes into the lower bay along the outer-bay channels, Niubi Channel and Fodu Channel. However, in the narrow middle and upper bay, hydrodynamics are generally controlled by gravitational circulation, with the outer bay water intruding at the bottom, while the inner-bay water flows out at the surface (Dong and Su. 2000; Xu et al., 2016) (Fig. 1b). The residence time of water in the lower bay is 5 to 15 days (for 90 % water exchange), and increases to approximately 60 days in the middle bay and approximately 80 days in the upper bay (Dong and Su, 1999).

## 2.2. Sampling strategy

Two cruises were conducted in XSB during the summer of 2017 (30 and 31, July) and the winter of 2019 (15 to 17, January). Both cruises were conducted during neap tide, without strong winds or precipitation. Surface (0.5 m depth) and bottom (1 m above the seabed) water were collected at 12 inner-bay stations (S1 to S12) using Niskin bottles, which were guided by a conductivity-temperature-depth (CTD) recorder (Sea-Bird). The in-situ temperature and salinity were measured directly on board. Based on the topography and hydrography, the stations are separated into four segments (Fig. 1b): (i) the upper bay segment (UB, including station S1, S2, S3, and S4); (ii) the middle bay segment (MB, including station S5, S6, S7 S10, and S11); (iii) the lower bay segment (LB, including station S12); and (iv) the Xihu Inlet segment (XI,

including station S8, S9). The temperature and salinity of the outer bay channels were also measured from the surface to the bottom at five sites during the winter cruise (Fig. 1b), whereas the summer outer bay datasets used in this study were published data obtained during the summer of 2007 (Zeng et al., 2011).

## 2.3. Measurements of nutrients and chlorophyll a

Water samples were filtered onboard through a pre-washed cellulose acetate membrane filter with a pore size of 0.45 µm. The ammonium (NH $_4^+$ ) concentration was measured onboard immediately after sampling, following the seawater-adapted indophenol blue spectrophotometric procedures, with a detection limit of 0.5 µmol L $^{-1}$  (Pai et al., 2001). Concentrations of nitrate plus nitrite (NO $_3^-$  + NO $_2^-$ ), DSi, and DIP were determined in the laboratory following the adapted standard spectrophotometric method (Grasshoff et al., 2009) on an AA3 autoanalyzer (SEAL Analytical GmbH, Norderstedt, Germany), with the water samples stored frozen ( $-20~^{\circ}\text{C}$ ) immediately after filtration. The detection limits for NO $_3^-$  + NO $_2^-$ , NO $_2^-$ , DSi, and DIP were 0.1, 0.04, 0.08, and 0.08 µmol L $^{-1}$ , respectively. The precisions estimated by repeated determinations of selected samples were  $\pm$  1 % for NO $_3^-$  + NO $_2^-$ , NO $_2^-$ , DSi,  $\pm$ 2 % for DIP, and  $\pm$  4 % for NH $_4^+$ . The concentration of DIN is defined as the sum of the NO $_3^-$ , NO $_2^-$ , and NH $_4^+$  concentrations.

Water samples for chlorophyll a (Chl-a) analysis were frozen immediately in liquid nitrogen after being filtered through 25 mm diameter GF/F filters (Whatman®, Maidstone, UK). The concentration of Chl-a was determined using a Turner Design®(San Jose, USA) Fluorometer fitted with a red-sensitive photomultiplier (Strickland and Parsons, 1972). The detection limit and precision are 0.025 mg  $\rm L^{-1}$  and  $\pm$  5 %, respectively.

All the reagents we used for the measurement were from Aladdin®, Shanghai, China.

## 2.4. Definition of the major nutrient sources

Nutrient dynamics in XSB are controlled by a multitude of processes and sources along the land-ocean aquatic continuum (Fang et al., 2021; Jiang et al., 2020; Ning and Hu, 2002; Peng et al., 2022; Yang et al., 2018). The three major sources are (i) the nutrients contributed by the external intrusion of the NEIW (eNut); (ii) the nutrients introduced by the inner-bay freshwater sources (fNut), including local river discharges with sewage and agricultural wastewater draining along the catchment, and submarine groundwater discharges; and (iii) the nutrients added or removed by regional processes not controlled by the transportation of the major water masses (rNut), including local point sources input (e.g. land-sea direct wastewater drainage), grazing or excessive feeding by aquaculture, internal biogenic consumption or regeneration, atmospheric deposition, and recycling from sediments and suspended particles.

## 2.5. Salinity-based conservative intrusion/mixing model

## 2.5.1. Outer bay intrusion model for eNut estimation

As a semi-enclosed bay with only one path connecting it with the outer bay water, the water masses in XSB are supplied by two major sources: local freshwater discharge and NEIW intrusion. Regulated by the seasonal variation in the CJR plume, the water masses of NEIW are generally constant on a seasonal scale (Wu et al., 2014), thus, the intrusion of the NEIW adjacent to the outer bay could be considered a conservative process with a residence time of the inner-bay water increasing from 10 to 80 days from lower bay to upper bay (Dong and Su, 1999). As the main source of saline water, a simplified conservative intrusion model based on the mass balance of salinity (Fig. 2a and b) was employed to express the contribution of the NEIW intrusion to XSB [Eq. (1) and Eq. (2)],

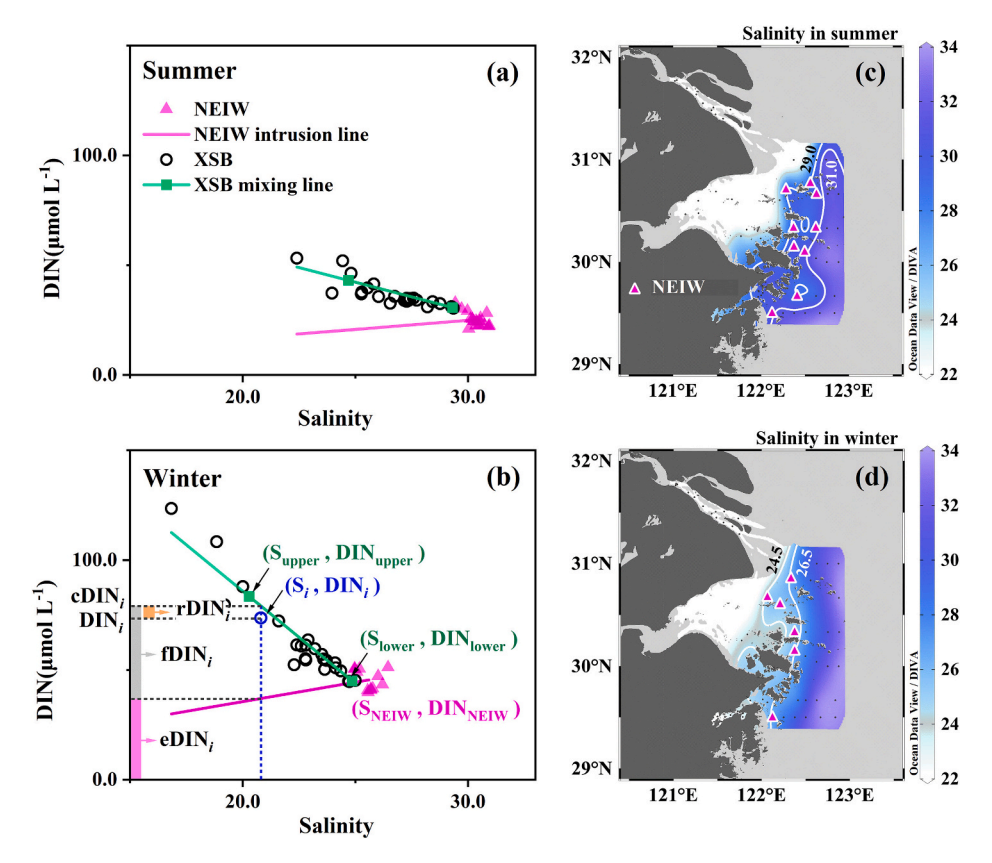


Fig. 2. The diagrams of the salinity-based conservative intrusion/mixing model (take DIN as an example). The relationship between the in-situ DIN concentration  $(\mu mol \ L^{-1})$  and salinity in XSB during (a) summer 2017 and (b) winter 2019 are shown by black circles. The upper bay endmember  $(S_{lupper}, DIN_{lupper})$  and lower bay endmember  $(S_{lower}, DIN_{lower})$  are shown by green squares, while the inner-bay conservative mixing line is indicated by the green solid line. The pink triangles in Figure (a) (b) indicate the NEIW endmember  $(S_{NEIW}, DIN_{NEIW})$ , while the pink solid line indicates the variation of the NEIW-derived DIN (eDIN) concentration with salinity, which was defined as the "NEIW intrusion line". A random water sample  $(S_{ib}, DIN_{i})$  during winter cruise (b) is marked with blue, with the contribution of eDIN<sub>is</sub> fDIN<sub>is</sub> and rDIN<sub>i</sub> to the in-situ DIN concentration marked on the axis of DIN concentration by pink, gray, and yellow shadow, respectively. The location of the NEIW endmember during (c) summer and (d) winter are marked on the map of the XSB adjacent coastal area, with the distribution of the water salinity at 8 m depth shown by the color gradient. The datasets of NEIW are collected from Ji (2016) and Wang et al. (2014).

$$f_0 + f_{\text{NEIW}} = 1 \tag{1}$$

$$f_0 S_0 + f_{\text{NEIW}} S_{\text{NEIW}} = S_{\text{in-situ}}$$
 (2)

where the fraction of the local freshwater discharge and intruded saline NEIW is represented by  $f_0$  and  $f_{\rm NEIW}$ , respectively.  $S_{\rm NEIW}$  represents the salinity of NEIW and  $S_{\rm in-situ}$  represents the in-situ salinity. The salinity of the internal freshwater ( $S_0$ ) equals 0, so that  $f_{\rm NEIW}$  can be expressed by Eq. (3). Hence, eNut for each study site can be estimated using  $f_{\rm NEIW}$  and the nutrient concentrations of NEIW ( $Nut_{\rm NEIW}$ ) [Eq. (4)],

$$f_{\text{NEIW}} = S_{\text{in-situ}} / S_{\text{NEIW}} \tag{3}$$

$$f_{\text{NEIW}} \text{ Nut}_{\text{NEIW}} = \text{eNut}$$
 (4)

Since the water in the outer bay channels is constantly occupied by adjacent NEIW (Dong and Su, 2000; Xu et al., 2016), the endmember of the intruding NEIW (Table 1) was defined along the ECS coastal water adjacent to the mouth of XSB depending on the salinity range of the outer bay channels, which was 29.0 to 31.0 in summer (Zeng et al., 2011), and 24.5 to 26.5 in winter (Fig. 3). The endmember of NEIW were defined with the data of the Chinese coastal investigation during 2006 and 2007 (Ji, 2016; Wang et al., 2014), and the selected sites representing the NEIW endmember during summer and winter are shown in Fig. 2c and d, respectively. The study sites affected by phytoplankton blooming (with dissolved oxygen saturation higher than 100 %) during the summer cruise were not included in the selection of the NEIW endmember. As shown in Fig. S1, the ranges of the selected NEIW

Table 1 Characteristics of endmember water masses in Xiangshan Bay. Values are reported as averages  $\pm$  one standard deviation.

Water masses	Season	Salinity	Nutrient con endmember ( $\mu$ mol L <sup>-1</sup> )	centration of t	he
Northern ECS		S <sub>NEIW</sub>	DIN <sub>NEIW</sub>	DSi <sub>NEIW</sub>	DIP <sub>NEIW</sub>
Inshore	Summer	30.3 ±	$24.6 \pm 4.4$	$25.2 \pm 3.2$	$0.68 \pm$
Water		0.4			0.18
(NEIW)	Winter	25.6 $\pm$	$39.3 \pm 5.4$	$\textbf{45.5} \pm \textbf{4.7}$	0.99 $\pm$
		0.5			0.14
Upper bay		$S_{upper}$	$DIN_{upper}$	$DSi_{upper}$	$DIP_{upper}$
water	Summer	24.7 $\pm$	$44.4 \pm 6.1$	$43.1 \pm 6.6$	$1.71~\pm$
		1.1			0.44
	Winter	20.3 $\pm$	83.5 $\pm$	65.7 $\pm$	1.84 $\pm$
		2.0	22.3	12.3	0.15
Lower bay		$S_{lower}$	$DIN_{lower}$	$DSi_{lower}$	$DIP_{lower}$
water	Summer	29.3 $\pm$	$26.1\pm0.4$	$30.7 \pm 0.5$	$0.90 \pm$
		0.1			0.01
	Winter	24.9 $\pm$	$\textbf{45.0} \pm \textbf{0.3}$	$40.0 \pm 0.1$	1.06 $\pm$
		0.2			0.04

endmember during summer and winter generally cover the range of the nutrient concentrations of the NEIW at the same salinity during July 2006, January 2007, August 2009, and August 2011, except for the extremely low nutrient concentrations during summer. With the dominating contribution of CJR nutrient loads, the diagrams of nutrients to salinity for the NEIW are generally on the linear dilution lines from the

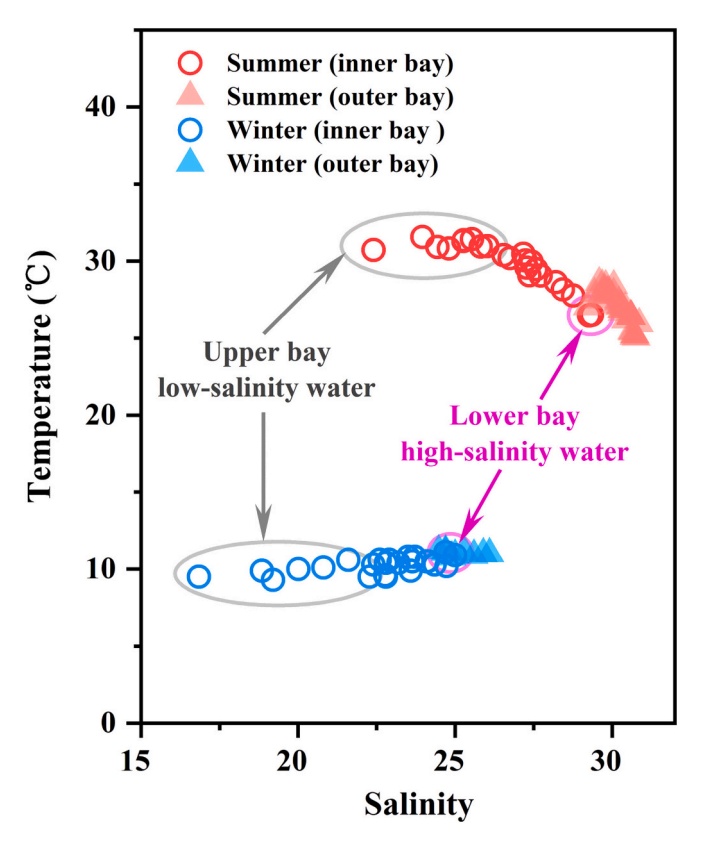


**Fig. 3.** The diagrams of temperature (°C) to salinity (T-S) of Xiangshan Bay (XSB). T-S diagrams during the 2017 summer and 2019 winter cruise are shown by red and blue hollow circles, respectively; the T-S diagrams of the outer bay channels of summer and winter are shown by red and blue triangles.

CJR mouth to the off-shore seawater, without significant seasonal and interannual variation. According to Chen et al. (2020), obvious change in the nutrient ranges in NEIW only happened on a decadal scale with the CJR nutrient loads accelerated from the 1980s to the 2010s. Since the nutrient loads of CJR were generally fluctuating at similar levels during the 2010s (Ran et al., 2022; Zhang et al., 2021), the nutrient concentrations of the NEIW with a salinity range of approximately 25 to 30 would fluctuate in a constant range.

## 2.5.2. Inner-bay mixing model and the estimation of rNut and fNut

As illustrated in the temperature-salinity (T-S) diagram (Fig. 3), the inner-bay mixing generally consisted of two distinguishable water masses: upper bay low-salinity water and lower bay high-salinity water. Water temperature is not considered a conservative indicator for source distinction, because it is significantly influenced by the heat exchange with the atmosphere and tidal flats in shallow coastal bays (Kong et al., 2022). Thus, the nutrient concentration mainly governed by inner bay mixing processes (cNut) is estimated with a simplified two-endmember mixing model (Han et al., 2012; Yang et al., 2018) (Fig. 2a and b). Because the inner-bay freshwater sources were concentrated and regionally well mixed in the upper bay with a relatively long residence time (Dong and Su, 1999), all UB stations (stations S1 to S4) were selected as the upper bay endmembers for the inner-bay mixing model, which was characterized by relatively low salinity and high nutrient concentrations. The LB station (station S12) was selected as the lower bay end member, characterized by higher salinity and lower nutrient concentrations, representing water transported upward into the bay from the lower bay area (Table 1). Salinity mass balance was used to calculate the water fractions of the upper bay endmember ( $f_{upper}$ ) and lower bay endmember ( $f_{lower}$ ) at each study site [Eq. (5) and Eq. (6)]:

$$f_{\text{upper}} + f_{\text{lower}} = 1 \tag{5}$$

$$f_{\text{upper}}S_{\text{upper}} + f_{\text{lower}}S_{\text{lower}} = S_{\text{in-situ}}$$
 (6)

where  $S_{upper}$  and  $S_{lower}$  represent the salinities of the upper and lower bay endmembers, respectively. Hence, cNut of each study site was estimated using the nutrient concentration and water fractions of the two endmembers [Eq. (7)]:

$$f_{\text{upper}} \text{Nut}_{\text{upper}} + f_{\text{lower}} \text{Nut}_{\text{lower}} = \text{cNut}$$
 (7)

where Nut<sub>upper</sub> and Nut<sub>lower</sub> represent the nutrient concentrations of the upper and lower bay endmember, respectively. The upper and lower bay endmembers were defined based on the T-S diagram (Fig. 3, Table 1).

rNut was defined as the difference between the in situ measured nutrient concentration (Nut<sub>in-situ</sub>) and cNut [Eq. (8)]. The negative (–) value of rNut indicates the amount of nutrient removed by processes such as biogenic consumption and adsorption by particulate matters; while the positive value indicates the nutrient added by regeneration, regional point source, and desorption from the particulate matters.

$$rNut = Nut_{in-situ} - cNut$$
 (8)

Because the water in the XSB consisted of the mixing of the local freshwater discharge and the NEIW intrusion, fNut was estimated by the difference between cNut and eNut [Eq. (9)].

$$fNut = cNut - eNut$$
 (9)

The uncertainties of eNut, fNut, and rNut caused by the uncertainties of the parameters in the endmembers were calculated using error propagation formulas (Han et al., 2021; Taylor, 1997) (details of the uncertainty calculation are outlined in S3), and the sum of the uncertainties was lower than the calculated result (Table 2).

## 2.6. Nutrient inventories estimation

Nutrient inventories contributed by eNut, fNut, and rNut were calculated by multiplying the concentrations with the water volume of each station unit. The area and average depth of each station were measured using an online sea chart (https://ais.msa.gov.cn/). The total inner bay nutrient inventories include all segments except LB.

## 2.7. Historical datasets

Nutrient concentrations of XSB during the recent four decades (from the 1980s to the 2010s) were collected from the literature (Fan and Jin, 1989; Hu et al., 1995; Jiang et al., 2019b; Jiang et al., 2013; Liu et al., 2000; Lü, 2015; Ning and Hu, 2002; Zeng et al., 2011; Zhang et al., 2007;

**Table 2**List of the concentration ranges for eNut, fNut, and rNut.

Season	Concentration range (µmol L <sup>-1</sup> )				
Summer	eDIN	eDSi	eDIP		
	18.6 to 24.4 (0.8)	18.2 to 23.8 (0.6)	0.50 to 0.66(0.08)		
	fDIN	fDSi	fDIP		
	6.3 to 30.6 (1.7)	2.2 to 35.2 (1.5)	0.23 to 1.61(0.25)		
	rDIN	rDSi	rDIP		
	-7.7 to 8.2 (0.9)	-6 to 3.2 (0.9)	-0.47 to 0.51(0.16)		
Winter	eDIN	eDSi	eDIP		
	29.9 to 44.4 (1.0)	25.9 to 38.4 (0.8)	0.65 to 0.96(0.09)		
	fDIN	fDSi	fDIP		
	0.0 to 82.6 (2.7)	0.8 to 59.2 (3.9)	0.07 to 1.77(0.36)		
	rDIN	rDSi	rDIP		
	-14.3 to 12.8 (1.7)	-6.7 to 4.2 (3.1)	-0.31 to 0.49(0.27)		

The estimated nutrient concentration ranges of eNut, fNut, and rNut are listed with the calculation uncertainty (Han et al., 2021; Taylor, 1997) in parentheses (details for the calculation uncertainty are outlined in S3). "—" represented the nutrient removal.

Zheng et al., 2000) (with the description of the collected data listed in Table S1).

#### 3. Results

## 3.1. Physico-chemical properties

The spatial distributions of water temperature and salinity during the two cruises are shown in Fig. 4a, b, g, and h. The summer water temperature of XSB varied from 26.5 to 31.6 °C, gradually decreasing

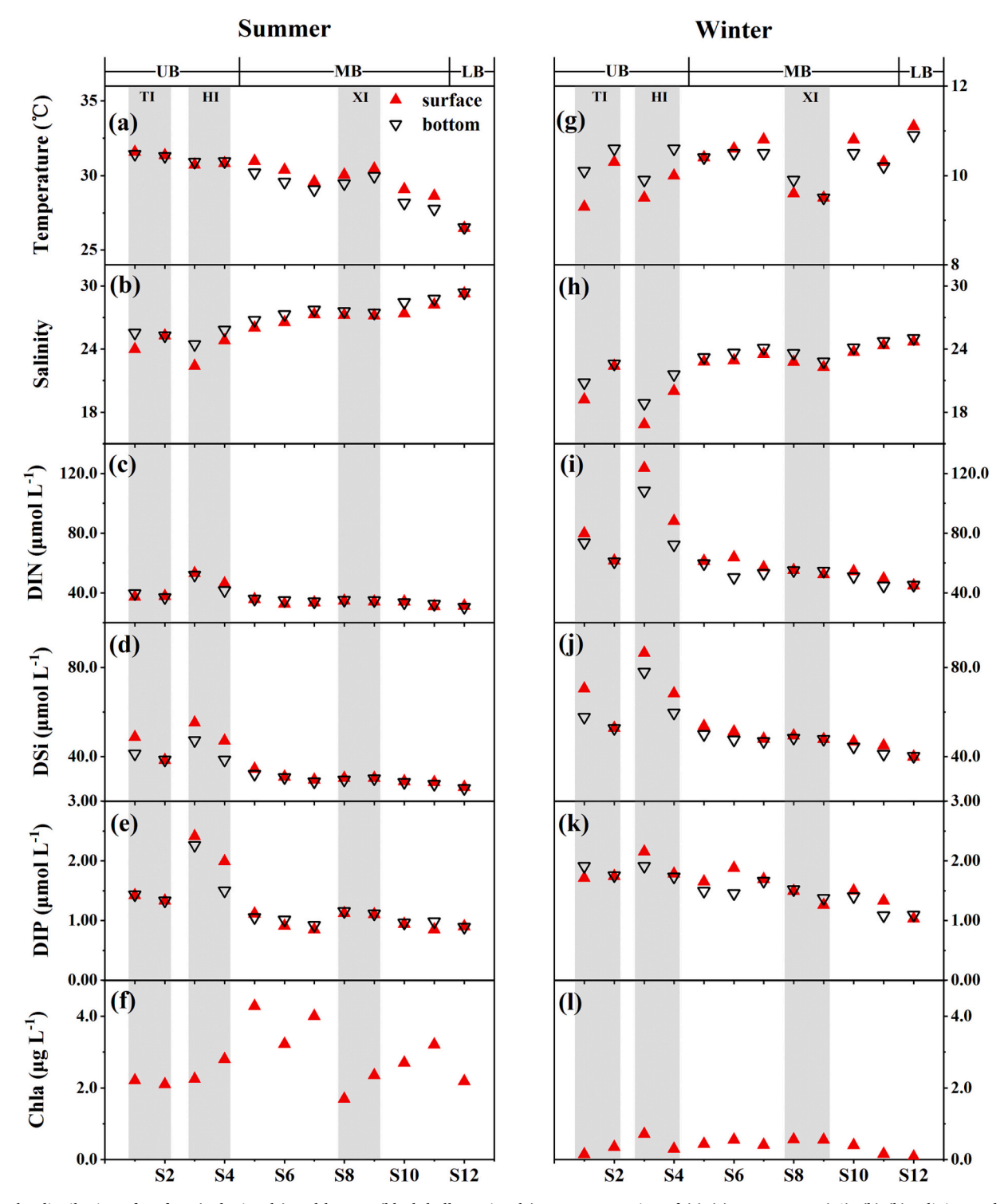


Fig. 4. The distribution of surface (red triangle) and bottom (black hollow triangle) water per station of (a) (g) temperature (°C), (b) (h) salinity, and the concentration of (c) (i) DIN ( $\mu$ mol L<sup>-1</sup>), (d) (j) DSi ( $\mu$ mol L<sup>-1</sup>), (e) (k) DIP ( $\mu$ mol L<sup>-1</sup>), and (f) (l) surface Chl-a ( $\mu$ g L<sup>-1</sup>) during the 2017 summer and 2019 winter cruises. The three branching bays (TI: Tie Inlet; HI: Huangdun Inlet; XI: Xihu Inlet) are displayed by gray shading. The ranges of upper bay (UB), middle bay (MB), and lower bay segment (LB) are marked on the top of the graphs.

outward from the shallow UB to the LB. While in winter, the range of water temperature was 9.3 to 11.1 °C, with the coldest water in the shallow branch bays, and warmer water in LB. On average, the summer water temperature (29.8  $\pm$  1.5 °C) was about 20 °C warmer than that in winter (10.2  $\pm$  0.5 °C). The salinity of XSB water was 22.4 to 29.4 in summer and decreased to 16.8 to 25.0 in winter. A decrease from LB to UB was observed in both seasons, with the salinity of the bottom water in LB always being the highest. The range of salinity in MB was 26.0 to 28.8 in summer and 22.8 to 24.7 in winter, with a downward decrease in both seasons. For UB, the water was fresher than MB with a wider range, which was 22.4 to 25.8 in summer and 16.8 to 22.6 in winter. The surface salinity was lower than that at the bottom by 2 at the heads of the TI and HI, indicating buoyant riverine freshwater discharge. In addition, the salinity in XI was slightly lower than that of the ambient MB water.

The spatial distribution trends of nutrient concentrations were similar during the summer and winter cruises; however, the values were much higher in winter, especially for DIN and DSi. In summer (Fig. 4c, d, and e), the concentration ranges for DIN, DSi, and DIP were 30.4 to 53.2  $\mu$ mol  $L^{-1},\ 25.9$  to  $55.2\ \mu$ mol  $L^{-1},\ and\ 0.85$  to  $2.41\ \mu$ mol  $L^{-1},\$ which increased to 60.9 to  $123.6\ \mu$ mol  $L^{-1},\ 52.7$  to  $86.4\ \mu$ mol  $L^{-1},\$ and 1.03 to  $2.15\ \mu$ mol  $L^{-1}$  in winter (Fig. 4i, j, and k), respectively. Matching with the low salinity, the nutrient levels in the UB were very high. The concentration of DIN, DSi, and DIP in UB was  $43.1\pm6.6\ \mu$ mol  $L^{-1},\ 44.4\pm6.1\ \mu$ mol  $L^{-1},\$ and  $1.71\pm0.44\ \mu$ mol  $L^{-1}$  in summer, while  $83.5\pm22.3\ \mu$ mol  $L^{-1},\ 65.7\pm12.3\ \mu$ mol  $L^{-1},\$ and  $1.84\pm0.15\ \mu$ mol  $L^{-1}$  in winter, respectively, with the highest nutrient concentrations constantly observed at the head of HI (station S3). The nutrient concentration decreased rapidly outward from UB to MB, where the concentration

range of DIN, DSi, and DIP was 31.0 to 35.8  $\mu mol~L^{-1}$ , 27.8 to 34.4  $\mu mol~L^{-1}$ , and 0.85 to 1.11  $\mu mol~L^{-1}$  in summer, while 44.7 to 63.6  $\mu mol~L^{-1}$ , 41.1 to 53.5  $\mu mol~L^{-1}$ , and 1.08 to 1.88  $\mu mol~L^{-1}$  in winter, respectively. The lowest nutrient values were observed in LB water, containing 30.7  $\pm$  0.5  $\mu mol~L^{-1}$  of DIN, 26.1  $\pm$  0.4  $\mu mol~L^{-1}$  of DSi, and 0.90  $\pm$  0.00  $\mu mol~L^{-1}$  of DIP in summer, and to 45.0  $\pm$  0.3  $\mu mol~L^{-1}$ , 40.0  $\pm$  0.1  $\mu mol~L^{-1}$ , and 1.06  $\pm$  0.04  $\mu mol~L^{-1}$  in winter, respectively. There was no vertical variation in the nutrient concentrations in the MB and LB in summer, whereas the surface values of the MB were slightly higher in winter. However, the nutrient concentration in UB was higher in the surface water than in the bottom water, especially in HI. The DIN consisted mainly of NO $_3^-$  in the whole bay and relatively high values of NO $_2^-$  and NH $_4^+$  were observed only in UB (Fig. S2).

The Chl-a concentration was much higher in summer (1.7 to 4.3  $\mu g$  L<sup>-1</sup>) than in winter, (0.1 to 0.7  $\mu g$  L<sup>-1</sup>). The highest Chl-a was observed in the upper MB during summer (Fig. 4f, and I).

## 3.2. Contribution of eNut, fNut, and rNut to the XSB nutrient inventory

Based on our calculations, the total inner-bay inventory of DIN, DSi, and DIP was  $124.0 \times 10^6$  mol,  $112.0 \times 10^6$  mol, and  $3.68 \times 10^6$  mol in summer, which was higher by >50 % in winter and amounted to 199.8  $\times 10^6$  mol,  $173.1 \times 10^6$  mol, and  $5.48 \times 10^6$  mol, respectively (Fig. 5a, b and c)

NEIW-derived eNut dominated the nutrient inventories in all parts of XSB. Seasonally, the inventory of eDIN, eDSi, and eDIP increased dramatically from  $82.3 \times 10^6$  mol,  $80.4 \times 10^6$  mol, and  $2.2 \times 10^6$  mol in summer, to  $151.9 \times 10^6$  mol,  $131.4 \times 10^6$  mol, and  $3.3 \times 10^6$  mol in

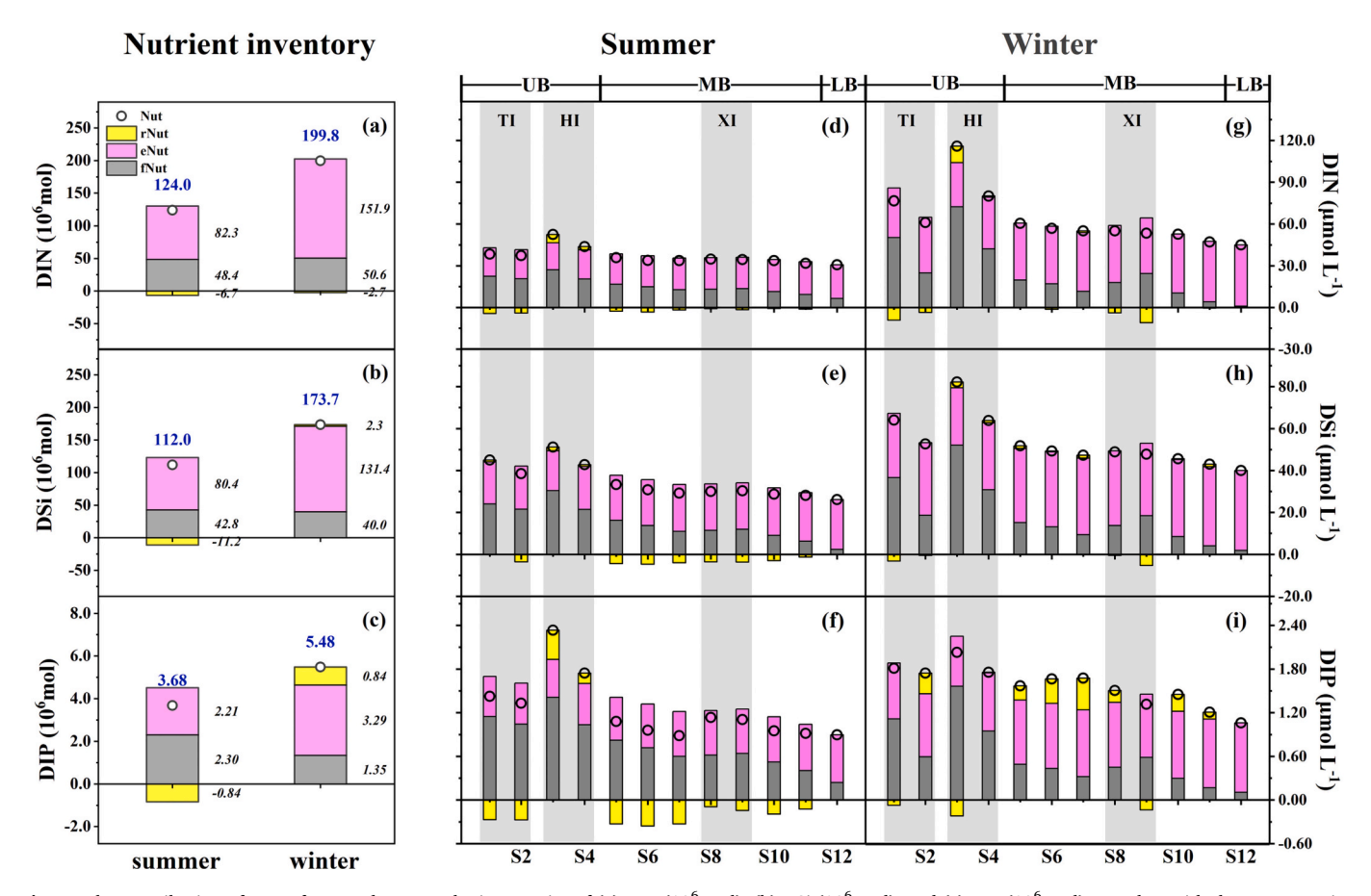


Fig. 5. The contribution of eNut, fNut, and rNut to the inventories of (a) DIN  $(10^6 \text{ mol})$ , (b) DSi  $(10^6 \text{ mol})$ , and (c) DIP  $(10^6 \text{ mol})$ , together with the concentration distribution per station of (d) (g) eDIN  $(\mu\text{mol }L^{-1})$ , fDIN  $(\mu\text{mol }L^{-1})$ , and rDIN  $(\mu\text{mol }L^{-1})$  (e) (h) eDSi  $(\mu\text{mol }L^{-1})$ , fDSi  $(\mu\text{mol }L^{-1})$ , and rDIN  $(\mu\text{mol }L^{-1})$ , fDIP  $(\mu\text{mol }L^{-1})$ , and rDIP  $(\mu\text{mol }L^{-1})$  during summer and winter. N represents the in situ nutrient concentration and inventory. The contribution of eNut, fNut, and rNut are displaied by pink, gray, and yellow columns, respectively.

winter. The contribution of eNut gradually increased outwards from the UB to the LB (Fig. 5d to 5i). In summer, the contribution percentage of eNut were 46 %, 45 %, and 31 % for DIN, DSi, and DIP in the UB, and 79 %, 91 %, and 73 % in the LB, respectively; in winter the contribution in the UB was almost similar to that in summer and increased to >90 % in the LB.

The inventory of local freshwater-derived fDIN and fDSi showed no seasonal variation, amounting to  $48.4 \times 10^6$  mol and  $42.8 \times 10^6$  mol in summer, and  $50.6 \times 10^6$  mol and  $40.0 \times 10^6$  mol in winter. In contrast, the fDIP inventory in summer ( $2.3 \times 10^6$  mol) was nearly twice as high as that in winter ( $1.3 \times 10^6$  mol), which was similar to that of eDIP. In contrast to eNut, the spatial distribution of the fNut contribution

decreased outwards from the UB to the MB, particularly in winter, indicating the accumulation of local freshwater-derived nutrients in the UB. In summer, the contributions of fDIN, fDSi, and fDIP to the UB were 50 %, 53 %, and 63 %, respectively, and decreased outward from 36 %, 33 %, and 49 % in MB to 21 %, 9 %, and 27 % in the LB, respectively; in winter, the contributions of fDIN, fDSi, and fDIP decreased outward from >50 % in the UB to about 20 % in the MB and <10 % in the LB.

The impact of the non-conservative rNut was limited to some areas without an apparent spatial gradient. In summer, rNut was negative at most of the stations, particularly in the MB. The total inventory of rDIN, rDSi, and rDIP was  $-6.7\times10^6$  mol,  $-11.2\times10^6$  mol, and  $-0.84\times10^6$  mol, indicating the nutrient removal processes. While, in winter, the

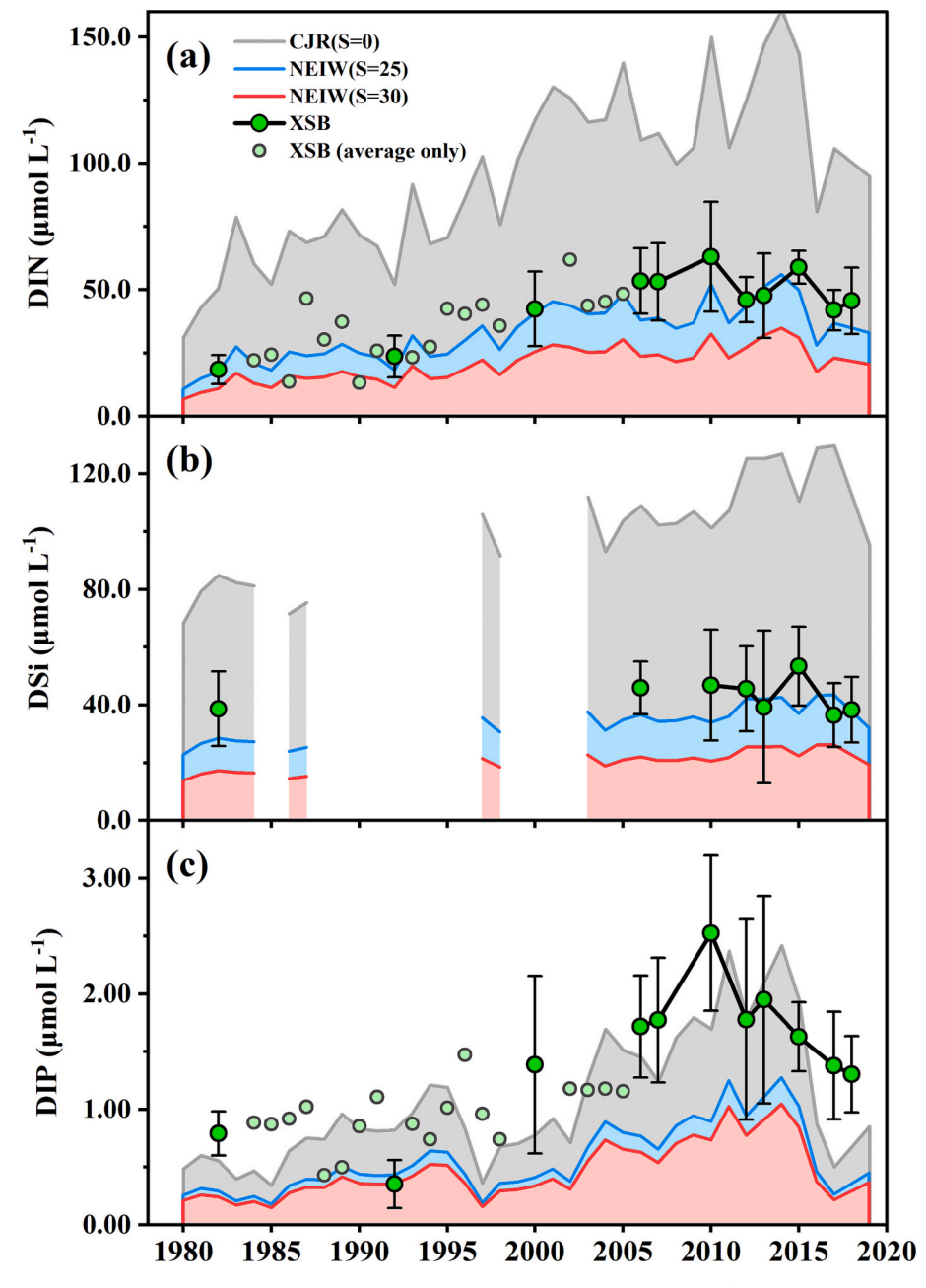


Fig. 6. The long-term trend of average nutrient concentrations in XSB and NEIW. Green circles indicate the annual average nutrient concentrations in the whole part of XSB with the standard deviation denoted by error bars (aver.  $\pm$  std.) (Fan and Jin, 1989; Jiang et al., 2019b; Jiang et al., 2013; Liu et al., 2000; Lü, 2015; Ning and Hu, 2002; Zeng et al., 2011); the light green circles without error bar indicate the years with only the annual average data published (Hu et al., 1995; Zhang et al., 2007; Zheng et al., 2000). Gray shading shows the average annual nutrient concentration of CJR mouth at 0 salinity (Li et al., 2007; Ran et al., 2022; Wang, 2006; Wang et al., 2021a; Xu et al., 2021; Zhang et al., 2021), while the blue and red shading indicates the NEIW nutrient concentrations at a salinity of 25 and 30, respectively.

general rDIN inventory decreased to  $-2.3 \times 10^6$  mol, and the inventory of rDSi and rDIP turned positive, amounting to  $2.7 \times 10^6$  mol and  $0.84 \times 10^6$  mol, respectively, indicating nutrient addition. The impact of rDIN and rDSi was apparent only in the branch bays, however, rDIP was positive for most stations, contributing 13 % of DIP to the TI, 22 % to the upper MB, and 12 % to the lower MB.

## 3.3. Long-term trend of the nutrient concentrations in XSB

The DIN concentration of XSB increased gradually from the 1980s to the 2000s by about 160 % and reached the climax in 2010 (63  $\pm$  22  $\mu mol~L^{-1}$ , Fig. 6a). In the 2010s there was no obvious trend, concentrations fluctuated around 40 to 60  $\mu mol~L^{-1}$ . The long-term pattern of DIP (Fig. 6c) in XSB similarly increased rapidly from the 1980s to the 2000s by about 140 %, reached the climax in 2010 (2.5  $\pm$  0.8  $\mu mol~L^{-1}$ ), and then decreased gradually during the 2010s. Unlike DIN and DIP, the DSi concentration of XSB (Fig. 6b) was constantly fluctuating at around 35 to 45  $\mu mol~L^{-1}$  in recent decades, with the highest value (53  $\pm$  2  $\mu mol~L^{-1}$ ) appearing in 2015.

## 4. Discussion

## 4.1. Predominant contribution of NEIW intrusion to XSB nutrient inventories

According to our calculations, eNut dominated the nutrient inventories, especially for DIN and DSi, contributing 63 % of DIN, 65 % of DSi, and 49 % of DIP in summer, whereas the contributions increased to 75 %, 75 %, and 60 % in winter. Because of the limited local freshwater discharge, the inner bay water is mainly supplied by NEIW intrusion (Gao et al., 1990; Yuan et al., 2014). Hence, the nutrient inventories of XSB are mainly controlled by the nutrients of intruded NEIW, which are strongly impacted by the southward transported CDW. In winter, with the majority of the CDW transported southward along the ZMCC, the NEIW is characterized by relatively lower salinity and higher nutrient concentrations (Wu et al., 2021; Zhang et al., 2022). In summer, with the major CJR plume extending northeastward off-shore, the southward

transportation of the CDW is relatively weak (Beardsley et al., 1985; Wu et al., 2014). The disappearance of the strong ZMCC in summer allows for more in-shelf seawater and possibly upwelled Taiwan Warm Current (TWC) water to contribute to the NEIW, diluting the impact of eutrophic CDW with low-nutrient seawater (Zhu et al., 2004) (Fig. 7). As the inventories of local-derived nutrients (the combination of fNut and rNut) did not display seasonal variation (Fig. 5a, b, and c), it is reasonable to believe that the much higher inner-bay inventories of DIN, DSi, and DIP in winter were controlled by the strengthened southward delivery of CDW.

# 4.2. Nutrient contribution by local draining and internal regeneration/removal process

Local freshwater discharge was the second-largest nutrient source for XSB, which supplied 37 % of DIN, 35 % of DSi, and 51 % of DIP in summer, and 25 % of DIN, 23 % of DSi, and 24 % of DIP in winter. With a long residence time of about 80 days and limited local riverine runoff. most of the local freshwater-derived nutrients accumulated in the shallow UB (Fig. 5d to i), apparently intensifying regional eutrophication as documented by the Chl-a concentration of 2.3  $\pm$  0.3  $\mu$ g L<sup>-1</sup>. In addition, as represented by rNut, the nutrients added or removed by local point sources and internal recycling were generally <10 % of the total inventory. Even so, this may cause rapid and intensive regional deviations. The value of rNut was negative for most of the stations in summer, especially in the upper MB (Fig. 4d, e, and f), where the highest concentration of Chl-a (3.5  $\pm$  0.6  $\mu$ g L<sup>-1</sup>) was observed (Fig. 4f), matching with the high frequency of phytoplankton blooms reported from the upper MB (Jiang et al., 2019b). However, in winter, negative rNut was found only in the upper XI and TI (Fig. 4g, h, and i), which was possibly related to uptake by kelp and oyster farming during the cold season (Jiang et al., 2019a; Jiang et al., 2020). Meanwhile, a positive rNut was constantly found in HI close to a sanitary sewage outlet, especially for DIP and DIN.

Interestingly, local-derived DIP was quantitatively more significant than DIN and DSi, similar to the contribution of NEIW intrusion. As reported for phosphorus-rich estuaries and bays (e.g., Scheldt and CJR

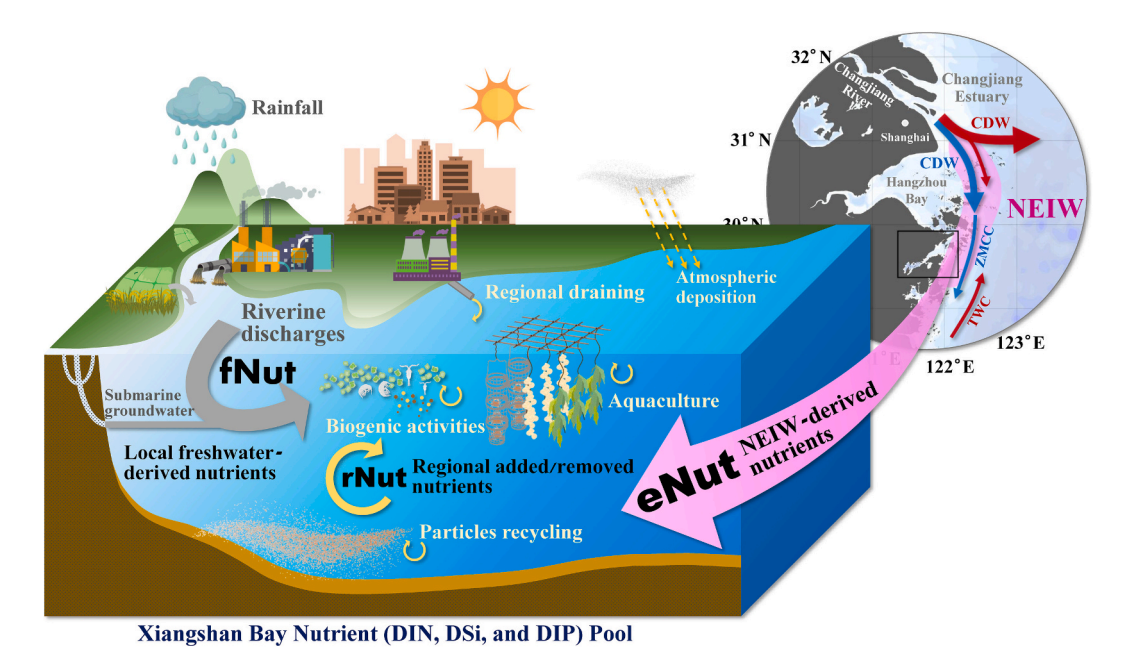


Fig. 7. Conceptual sketch of the processes controlling the nutrients in XSB. The nutrient inputs by outer bay coastal water intrusion (eNut), local freshwater discharging (fNut), and regional additional/removal processes (rNut) are displayed by pink, gray, and yellow arrows, respectively. The currents contributing to the northern part of the East China Sea (ECS) coastal waters (NEIW) are shown on the map. In summer (red arrows), the southward Changjiang Diluted Water (CDW) is relatively weak and mixes with the residual coastal seawater and possibly the upwelling-fueled northward Taiwan Warm Current (TWC). In winter (blue arrows), the majority of the CDW flows southward, extending into the Zhe-Min Coastal Current (ZMCC).

estuary) (van der Zee et al., 2007; Xu et al., 2015), most of the inner-bay DIP was trapped in the local area, where the higher salinity triggered the release of DIP that was adsorbed onto the surface of suspended particles and sediments, while the high turbidity at the bay mouth significantly absorbed the exported DIP. Besides, according to the estimation by Nobre et al. (2010) and Wu et al. (2017), the land-derived P/N ratio in XSB (0.08 to 0.11) was much higher than the DIP/DIN ratio of the nutrient inventories in XSB (0.030 in summer and 0.027 in winter), indicating a surplus land-derived P supply in XSB. The additional innerbay DIP supplementation released the P limitation of the intruded NEIW (Chen et al., 2020; Xu et al., 2015), thereby supporting the high frequency of large-cell phytoplankton blooms and increased deposition of organic matter during warm seasons (Jiang et al., 2019b).

## 4.3. Persistent effect of the CJR discharge on the XSB nutrients

The long-term variation in XSB nutrients is generally synchronous with that of the downstream CJR portion (Li et al., 2007; Ran et al., 2022; Wang, 2006; Wang et al., 2021a; Xu et al., 2021; Zhang et al., 2021) (Fig. 6). The nutrient concentrations of the NEIW adjacent to the outer bay were estimated assuming linear dilution from the CJR mouth to the ECS coastal water when the salinity was approximately 25 to 30 (the general salinity range of the XSB outer bay water) (described in S5). Deviations exist between the true values of the long-term nutrient concentrations of NEIW and the estimated values using a simplified linear dilution coefficient because of the temperate processes, such as biogenic activities and recycling of the legacy nutrients, however, the trend of the approximate nutrient concentrations in NEIW on the interannual scale could still be revealed in this way. The DIN and DSi concentrations in NEIW generally comprised 50 % to 90 % of those in XSB, indicating the persistent dominance of NEIW fed by CJR discharge (Fig. 6a and b). The DIP concentration of NEIW was approximately 40 % to 50 % of that of XSB, indicating a similar contribution of local and remote DIP sources (Fig. 6c).

The DIN and DIP of CJR increased from the 1980s to the 2000s and reached a peak from 2010 to 2015, owing to the accelerating anthropogenic activities (e.g., industrial and agricultural productions and domestic sewage draining) along river basin with rapid economic and social development in China (Wang et al., 2018; Zhang et al., 2021); while the DSi concentration did not display a temporal trend under the combined effects of dam building and the change of weathering (Ran et al., 2022). The observed decrease in DIN and DIP in the CJR in the late 2010s was likely related to policies and management focusing on the systemic restoration of the CJR basin since the mid-2010s, particularly in terms of fertilizer use reduction (Sills et al., 2020; Zhang et al., 2021). With the systematic consideration of land-use change in the CJR catchment and the sewage draining of downstream megacities such as Shanghai (Zhang et al., 2021) by policy and management, the nutrient input from the CJR into coastal waters will likely remain at a lower level or even be reduced further in the future.

## 4.4. Implication for eutrophication management

In the case of XSB, fed by large river discharge, the intruded outer bay coastal water is not the "solution" (by dilution) to eutrophication as in many other cases, but it is instead the main cause for the nutrient accumulation in such a narrow bay (Fig. 7). Because of their morphology and physical setting, semi-enclosed bays with a rather long water residence time can act as an amplifier of the coastal eutrophication driven by large river discharges, that is, a high frequency of HAB and ecosystem degradation (Du et al., 2020; Jiang et al., 2019b). As in XSB, the coastal bays under the cover of the CJR alongshore transportation are also suffering from severe eutrophication problems, including Hangzhou Bay, Sanmen Bay, Yueqing Bay, and possibly Sansha Bay, (Gao et al., 2022; Wang et al., 2021b; Wu et al., 2019; Zhu et al., 2022), in which the nutrients supplied by of the intruded coastal water fed by CJR discharge

should be carefully considered for local management.

The alongshore long-distance transport of the world's large riverdiluted water is a permanent feature with seasonal variations in direction and flux, regulated by wind force, tidal current, Ekman transport, and runoff variation (Horner-Devine et al., 2015). Significant remote effects of large river discharges also exist along the northwestern coast of the Gulf of Mexico fed by the Mississippi-Atchafalaya River discharge, the impact of which can extend westward over 600 km along the Louisiana-Texas shelf, transporting nutrient-laden water to the mouth of Terrebonne Bay, Fourleague Bay, and possibly Galveston Bay with decreasing local freshwater discharges (Bugica et al., 2020; Lane et al., 2010; Turner et al., 2012; Zhang et al., 2012). The plums of the Peal River, China, together with the coastal land input, can also extend along the Guangdong Coastal Current, reaching Zhanjiang Bay, approximately 360 km west of the river mouth, where the local freshwater discharge decreased, and the contribution of the outer-bay intruded water was 89 % in summer and 94 % in winter (Lao et al., 2022a). Research about the water mass alongshore transport driven by large river discharges revealed the fact that the nutrient-laden water can reach the mouth of the bays over hundreds of kilometers away from the large river estuary (Lao et al., 2022b; Yang et al., 2018; Zhang et al., 2012). With limited local freshwater input, the intrusion of the coastal water becomes the major water source for a semi-enclosed coastal bay, which can also be an important nutrient source for the local water. The eutrophication of coastal bays governed by the far-reaching effect of large river discharge may be a worldwide phenomenon of local importance that has gained much less attention than the large-scale direct effects of major world river inputs. Therefore, a quantitative understanding of the far-reaching effect of the world's large river discharges on coastal bays of such type is necessary for managers to consider local eutrophication mitigation in a wider context.

## 5. Conclusions

This study proved the hypothesis that the nutrient inventories in Xiangshan Bay, especially for DIN and DSi, are dominantly driven by the intrusion of NEIW fed by the southward alongshore transport of the Changjiang discharge, which is strengthened in winter. The contribution of the local sources is relatively more important to DIP than to DIN and DSi. In such a semi-enclosed bay with a rather long water residence time of weeks to months, eutrophication would be much enhanced with relatively stable water flow and the accumulation of both remote- and local-derived nutrients. Strict regulation of local sewage draining and the ameliorative integrated multi-trophic aquaculture are no doubt positive actions for nutrient reductions on a regional scale, however, practices limited on the local scale are not enough to mitigate the eutrophication in the coastal bays under the impact of a remote large river discharge, which can extend alongshore through hundreds of kilometers with nutrient-laden water. Therefore, inter-regional management depending on long-term monitoring, quantitative modeling, and systematic nutrient source tracing is urgently needed to mitigate the eutrophication in coastal bays like XSB.

## CRediT authorship contribution statement

Xiangyu Sun: Conceptualization, Investigation, Methodology, Visualization, Writing – original draft. Jingjing Zhang: Conceptualization, Investigation, Writing – review & editing. Hongliang Li: Conceptualization, Funding acquisition, Methodology, Supervision, Writing – review & editing. Yong Zhu: Investigation, Methodology. Xingju He: Data curation, Investigation. Yibo Liao: Investigation, Resources. Zhibing Jiang: Investigation, Resources. Lu Shou: Investigation, Resources. Zhiwen Wang: Data curation, Investigation. Tim C. Jennerjahn: Conceptualization, Writing – review & editing. Jianfang Chen: Conceptualization, Funding acquisition, Supervision.

#### Declaration of competing interest

The authors declare that they have no known competing financial interests or personal relationships that could have appeared to influence the work reported in this paper.

#### Data availability

Data will be made available on request.

#### Acknowledgements

This work was supported by the Key R&D Program of Zhejiang [grant number 2022C03044]; the Natural Science Foundation of Zhejiang [grant number LDT23D06023D06]; and the Scientific Research Fund of the Second Institute of Oceanography, MNR [grant number JG2214]. We thank Aiqin Han (Third Institute of Oceanography, Ministry of Natural Resources) for her suggestions on this study.

## Appendix A. Supplementary data

Supplementary data to this article can be found online at https://doi.org/10.1016/j.scitotenv.2023.168875.

#### References

- Anderson, D.M., Glibert, P.M., Burkholder, J.M., 2002. Harmful algal blooms and eutrophication: nutrient sources, composition, and consequences. Estuaries 25 (4), 704–726. https://doi.org/10.1007/BF02804901.
- Beardsley, R.C., Limeburner, R., Yu, H., Cannon, G.A., 1985. Discharge of the Changjiang (Yangtze river) into the East China Sea. Cont. Shelf Res. 4 (1–2), 57–76. https://doi.org/10.1016/0278-4343(85)90022-6.
- Boesch, D.F., 2019. Barriers and bridges in abating coastal eutrophication. Front. Mar. Sci. 6, 123. https://doi.org/10.3389/fmars.2019.00123.
- Bugica, K., Sterba-Boatwright, B., Wetz, M.S., 2020. Water quality trends in Texas estuaries. Mar. Pollut. Bull. 152, 110903 https://doi.org/10.1016/j.marnolbul.2020.110903
- Chen, J., Li, D., Jin, H., Jiang, Z., Wang, B., Wu, B., Hao, Q., Sun, X., 2020. In: Chen, C.-T. A., X., G. (Eds.), Changing Asia-Pacific Marginal Seas. Springer Nature Singapore Pte Ltd., Singapore, pp. 155–178. https://doi.org/10.1007/978-981-15-4886-4\_10.
- Cloern, J.E., Schraga, T.S., Nejad, E., Martin, C., 2020. Nutrient status of San Francisco Bay and its management implications. Estuar. Coasts 43 (6), 1299–1317. https://doi. org/10.1007/s12237-020-00737-w.
- Conley, D.J., Paerl, H.W., Howarth, R.W., Boesch, D.F., Seitzinger, S.P., Havens, K.E., Lancelot, C., Likens, G.E., 2009. Controlling eutrophication: nitrogen and phosphorus. Science 323 (5917), 1014–1015. https://doi.org/10.1126/ physics.phys
- Dong, L., Su, J., 1999. Numerical study of water exchange in Xiangshan Bay II. Model application and water exchange study. Oceanol. et Limnol. Sin. 4, 410–415 (In Chinese with English abstract).
- Dong, L., Su, J., 2000. Salinity distribution and mixing in Xiangshan bay I: salinity distribution and circulation pattern. Oceanol. et Limnol. Sin./Haiyang Yu Huzhao 31 (2), 151–158 (In Chinese with English abstract).
- Du, P., Jiang, Z., Zhu, Y., Tang, Y., Liao, Y., Chen, Q., Zeng, J., Shou, L., 2020. What factors control the variations in abundance, biomass, and size of mesozooplankton in a subtropical eutrophic bay? Estuar. Coasts 43 (8), 2128–2140. https://doi.org/10.1007/s12937.020.00747.8
- Duarte, C.M., Krause-Jensen, D., 2018. Intervention options to accelerate ecosystem recovery from coastal eutrophication. Front. Mar. Sci. 5, 470. https://doi.org/ 10.3389/fmars.2018.00470.
- Fan, A., Jin, X., 1989. Tidal effect on nutrient exchange in Xiangshan Bay, China. Mar. Chem. 27 (3–4), 259–281. https://doi.org/10.1016/0304-4203(89)90051-0.
- Fang, J., Zhang, J., Xiao, T., Huang, D., Liu, S., 2016. Integrated multi-trophic aquaculture (IMTA) in Sanggou Bay, China. Aquac. Environ. Interact. 8, 201–205. https://doi.org/10.3354/aei00179.
- Fang, X., Wang, Q., Wang, J., Xiang, Y., Wu, Y., Zhang, Y., 2021. Employing extreme value theory to establish nutrient criteria in bay waters: a case study of Xiangshan Bay. J. Hydrol. 603, 127146 https://doi.org/10.1016/j.jhydrol.2021.127146.
- Gaillardet, J., Dupré, B., Louvat, P.L., Allegre, C.J., 1999. Global silicate weathering and CO2 consumption rates deduced from the chemistry of large rivers. Chem. Geol. 159 (1–4), 3–30. https://doi.org/10.1016/S0009-2541(99)00031-5.
- Galloway, J.N., Townsend, A.R., Erisman, J.W., Bekunda, M., Cai, Z., Freney, J.R., Martinelli, L.A., Seitzinger, S.P., Sutton, M.A., 2008. Transformation of the nitrogen cycle: recent trends, questions, and potential solutions. Science 320 (5878), 889–892. https://doi.org/10.1126/science.1136674.
- Gao, S., Xie, Q., Feng, Y., 1990. Fine-grained sediment transport and sorting by tidal exchange in Xiangshan Bay, Zhejiang, China. Estuar. Coast. Shelf Sci. 31 (4), 397–409. https://doi.org/10.1016/0272-7714(90)90034-O.

- Gao, Y., Jiang, Z., Chen, Y., Liu, J., Zhu, Y., Liu, X., Sun, Z., Zeng, J., 2022. Spatial variability of phytoplankton and environmental drivers in the turbid Sammen Bay (East China Sea). Estuar. Coasts 45 (8), 2519–2533. https://doi.org/10.1007/s12937.022.01104.7
- Grasshoff, K., Kremling, K., Ehrhardt, M., 2009. Methods of Seawater Analysis. John Wiley & Sons, Germany, pp. 193–198. https://doi.org/10.1002/9783527613984.
- Greening, H., Janicki, A., Sherwood, E.T., Pribble, R., Johansson, J.O.R., 2014.
  Ecosystem responses to long-term nutrient management in an urban estuary: Tampa Bay, Florida, USA. Estuar. Coast. Shelf Sci. 151, A1–A16. https://doi.org/10.1016/j.ecss.2014.10.003.
- Hallegraeff, G.M., 1993. A review of harmful algal blooms and their apparent global increase. Phycologia 32 (2), 79–99. https://doi.org/10.2216/i0031-8884-32-2-79.
- Han, A., Dai, M., Kao, S.-J., Gan, J., Li, Q., Wang, L., Zhai, W., Wang, L., 2012. Nutrient dynamics and biological consumption in a large continental shelf system under the influence of both a river plume and coastal upwelling. Limnol. Oceanogr. 57 (2), 486–502. https://doi.org/10.4319/lo.2012.57.2.0486.
- Han, A., Kao, S.J., Lin, W., Lin, Q., Han, L., Zou, W., Tan, E., Lai, Y., Ding, G., Lin, H., 2021. Nutrient budget and biogeochemical dynamics in Sansha Bay, China: a coastal bay affected by intensive mariculture. J. Geophys. Res. Biogeosci. 126 (9), e2020JG006220 https://doi.org/10.1029/2020jg006220.
- Horner-Devine, A.R., Hetland, R.D., MacDonald, D.G., 2015. Mixing and transport in Coastal River plumes. Annu. Rev. Fluid Mech. 47 (1), 569–594. https://doi.org/ 10.1146/annurev-fluid-010313-141408.
- Hu, W., Chen, T., Xin, Y., Li, Z., 1995. The assessment on the environment monitoring of Xiangshan port. Mar. Environ. Sci. 14 (4), 57–63 (In Chinese with English abstract).
- Humborg, C., Ittekkot, V., Cociasu, A., Bodungen, B.V., 1997. Effect of Danube River dam on Black Sea biogeochemistry and ecosystem structure. Nature 386, 385–388. https://doi.org/10.1038/386385a0.
- Ji, W. (Ed.), 2016. Chinese Coastal Ocean-Marian Chemistry. Ocean Press, Beijing, China, pp. 7–44 (In Chinese).
- Jiang, Z., Zhu, X., Gao, Y., Chen, Q., Zeng, J., Zhu, G., 2013. Spatio-temporal distribution of net-collected phytoplankton community and its response to marine exploitation in Xiangshan Bay. Chin. J. Oceanol. Limnol. 31 (4), 762–773. https://doi.org/10.1007/ s00343-013-2206-z.
- Jiang, Z., Du, P., Liao, Y., Liu, Q., Chen, Q., Shou, L., Zeng, J., Chen, J., 2019a. Oyster farming control on phytoplankton bloom promoted by thermal discharge from a power plant in a eutrophic, semi-enclosed bay. Water Res. 159, 1–9. https://doi.org/ 10.1016/j.watres.2019.04.023.
- Jiang, Z., Du, P., Liu, J., Chen, Y., Zhu, Y., Shou, L., Zeng, J., Chen, J., 2019b.
  Phytoplankton biomass and size structure in Xiangshan Bay, China: current state and historical comparison under accelerated eutrophication and warming. Mar. Pollut. Bull. 142, 119–128. https://doi.org/10.1016/j.marpolbul.2019.03.013.
- Jiang, Z., Liu, J., Li, S., Chen, Y., Du, P., Zhu, Y., Liao, Y., Chen, Q., Shou, L., Yan, X., Zeng, J., Chen, J., 2020. Kelp cultivation effectively improves water quality and regulates phytoplankton community in a turbid, highly eutrophic bay. Sci. Total Environ. 707, 135561 https://doi.org/10.1016/j.scitotenv.2019.135561.
- Kong, G., Li, L., Guan, W., 2022. Influences of tidal flat and thermal discharge on heat dynamics in Xiangshan Bay. Front. Mar. Sci. 9, 850672 https://doi.org/10.3389/ fmars 2022 850672.
- Lane, R.R., Madden, C.J., Day, J.W., Solet, D.J., 2010. Hydrologic and nutrient dynamics of a coastal bay and wetland receiving discharge from the Atchafalaya River. Hydrobiologia 658 (1), 55–66. https://doi.org/10.1007/s10750-010-0468-4.
- Hydrobiologia 658 (1), 55–66. https://doi.org/10.1007/s10750-010-0468-4.

  Lao, Q., Liu, S., Ling, Z., Jin, G., Chen, F., Chen, C., Zhu, Q., 2023. External dynamic mechanisms controlling the periodic offshore blooms in Beibu Gulf. J. Geophys. Res. Oceans 128 (6), e2023JC019689. https://doi.org/10.1029/2023jc019689.
- Lao, Q., Wu, J., Chen, F., Zhou, X., Li, Z., Chen, C., Zhu, Q., Deng, Z., Li, J., 2022a. Increasing intrusion of high salinity water alters the mariculture activities in Zhanjiang Bay during the past two decades identified by dual water isotopes. J. Environ. Manag. 320, 115815 https://doi.org/10.1016/j.jenvman.2022.115815.
- Lao, Q., Zhang, S., Li, Z., Chen, F., Zhou, X., Jin, G., Huang, P., Deng, Z., Chen, C., Zhu, Q., Lu, X., 2022b. Quantification of the seasonal intrusion of water masses and their impact on nutrients in the Beibu Gulf using dual water isotopes. J. Geophys. Res. Oceans 127 (7), e2021JC018065. https://doi.org/10.1029/2021jc018065.
- Li, M., Xu, K., Watanabe, M., Chen, Z., 2007. Long-term variations in dissolved silicate, nitrogen, and phosphorus flux from the Yangtze River into the East China Sea and impacts on estuarine ecosystem. Estuar. Coast. Shelf Sci. 71 (1–2), 3–12. https://doi.org/10.1016/j.ecss.2006.08.013.
- Liu, X., Beusen, A.H.W., Van Beek, L.P.H., Mogollon, J.M., Ran, X., Bouwman, A.F., 2018. Exploring spatiotemporal changes of the Yangtze River (Changjiang) nitrogen and phosphorus sources, retention and export to the East China Sea and Yellow Sea. Water Res. 142, 246–255. https://doi.org/10.1016/j.watres.2018.06.006.
- Liu, Z., Cai, Y., Shi, J., Ning, X., 2000. Standing stock of phytoplankton and primary productivity in Penaeus orientalis larval multiplication releasing area of the Xiangshan Bay. Acta Oceanol. Sin. 19 (1), 109–118. http://aosocean.com/article/id/ 20000111.
- Lü, H. (Ed.), 2015. The Environmental Evaluation and Development of Xiangshan Bay. Ocean Press, Beijing, China, pp. 38–46 (In Chinese).
- Murphy, R.R., Keisman, J., Harcum, J., Karrh, R.R., Lane, M., Perry, E.S., Zhang, Q., 2022. Nutrient improvements in Chesapeake Bay: direct effect of load reductions and implications for coastal management. Environ. Sci. Technol. 56 (1), 260–270. https://doi.org/10.1021/acs.est.1c05388.
- Ning, X., Hu, X., 2002. Aquacultural Ecology and Carrying Capacity Assessment of Fish Cages in Xiangshan Bay. Ocean Press, Beijing, China, p. 132 (In Chinese).
- Nixon, S.W., 1995. Coastal marine eutrophication: a definition, social causes, and future concerns. Ophelia 41 (1), 199–219. https://doi.org/10.1080/ 00785236.1995.10422044.

- Nobre, A.M., Ferreira, J.G., Nunes, J.P., Yan, X., Bricker, S., Corner, R., Groom, S., Gu, H., Hawkins, A.J.S., Hutson, R., Lan, D., Lencart e Silva, J.D., Pascoe, P., Telfer, T., Zhang, X., Zhu, M., 2010. Assessment of coastal management options by means of multilayered ecosystem models. Estuar. Coast. Shelf Sci. 87 (1), 43–62. https://doi. org/10.1016/j.ecss.2009.12.013.
- Pai, S.-C., Tsau, Y.-J., Yang, T.-I., 2001. pH and buffering capacity problems involved in the determination of ammonia in saline water using the indophenol blue spectrophotometric method. Anal. Chim. Acta 434 (2), 209–216. https://doi.org/ 10.1016/S0003-2670(01)00851-0.
- Peng, T., Liu, J., Yu, X., Zhang, F., Du, J., 2022. Assessment of submarine groundwater discharge (SGD) and associated nutrient subsidies to Xiangshan Bay (China), an aquaculture area. J. Hydrol. 610, 127795 https://doi.org/10.1016/j. ihydrol.2022.127795.
- Ran, X., Wu, W., Song, Z., Wang, H., Chen, H., Yao, Q., Xin, M., Liu, P., Yu, Z., 2022. Decadal change in dissolved silicate concentration and flux in the Changjiang (Yangtze) river. Sci. Total Environ. 839, 156266 https://doi.org/10.1016/j. scitotenv.2022.156266.
- Schindler, D.W., 2006. Recent advances in the understanding and management of eutrophication. Limnol. Oceanogr. 51 (1part2), 356–363. https://doi.org/10.4319/ lo.2006.51.1 part 2.0356.
- Seitzinger, S.P., Harrison, J.A., Dumont, E., Beusen, A.H.W., Bouwman, A.F., 2005. Sources and delivery of carbon, nitrogen, and phosphorus to the coastal zone: an overview of global nutrient export from watersheds (NEWS) models and their application. Glob. Biogeochem. Cycles 19 (4), GB4S01. https://doi.org/10.1029/ 2005eb002606.
- Sills, J., Mei, Z., Cheng, P., Wang, K., Wei, Q., Barlow, J., Wang, D., 2020. A first step for the Yangtze. Science 367 (6484), 1314. https://doi.org/10.1126/science.abb5537.
- Strickland, J.D.H., Parsons, T.R., 1972. A practical handbook of seawater analysis. In: Bulletin of the Fisheries Research Board of Canada, p. 310. https://doi.org/10.25607/OBP-1791. Ottawa, Canada.
- Strokal, M., Yang, H., Zhang, Y., Kroeze, C., Li, L., Luan, S., Wang, H., Yang, S., Zhang, Y., 2014. Increasing eutrophication in the coastal seas of China from 1970 to 2050. Mar. Pollut. Bull. 85 (1), 123–140. https://doi.org/10.1016/j.marpolbul.2014.06.011.
- Taylor, J., 1997. Introduction to Error Analysis, the Study of Uncertainties in Physical Measurements. University Science Books, New York, USA, p. 328.
- Turner, R.E., Rabalais, N.N., Justic, D., 2012. Predicting summer hypoxia in the northern Gulf of Mexico: redux. Mar. Pollut. Bull. 64 (2), 319–324. https://doi.org/10.1016/j.marpolbul.2011.11.008.
- van der Zee, C., Roevros, N., Chou, L., 2007. Phosphorus speciation, transformation and retention in the Scheldt estuary (Belgium/the Netherlands) from the freshwater tidal limits to the North Sea. Mar. Chem. 106 (1–2), 76–91. https://doi.org/10.1016/j. marchem.2007.01.003.
- Wang, B., 2006. Cultural eutrophication in the Changjiang (Yangtze River) plume: history and perspective. Estuar. Coast. Shelf Sci. 69 (3–4), 471–477. https://doi.org/ 10.1016/j.ecss.2006.05.010.
- Wang, K., Chen, J., Jin, H., Li, H., Gao, S., Xu, J., Lu, Y., Huang, D., Hao, Q., Weng, H., 2014. Summer nutrient dynamics and biological carbon uptake rate in the Changjiang River plume inferred using a three end-member mixing model. Cont. Shelf Res. 91, 192–200. https://doi.org/10.1016/j.csr.2014.09.013.
- Wang, K., Cai, W.-J., Chen, J., Kirchman, D., Wang, B., Fan, W., Huang, D., 2021a. Climate and human-driven variability of summer hypoxia on a large river-dominated shelf as revealed by a hypoxia index. Front. Mar. Sci. 8, 634184 https://doi.org/ 10.3389/fmars.2021.634184
- Wang, Y., Liu, D., Xiao, W., Zhou, P., Tian, C., Zhang, C., Du, J., Guo, H., Wang, B., 2021b. Coastal eutrophication in China: trend, sources, and ecological effects. Harmful Algae 107, 102058. https://doi.org/10.1016/j.hal.2021.102058.
- Wu, R., Wu, H., Wang, Y., 2021. Modulation of shelf circulations under multiple river discharges in the East China Sea. J. Geophys. Res. Oceans 126 (4), e2020JC016990. https://doi.org/10.1029/2020jc016990.
- Wu, Z., Zhou, H., Zhang, S., Liu, Y., 2013. Using 222Rn to estimate submarine groundwater discharge (SGD) and the associated nutrient fluxes into Xiangshan Bay, East China Sea. Marine Poll. Bull. 73 (1), 183–191. https://doi.org/10.1016/j. marpolbul.2013.05.024.

- Wu, Y., Li, D., Ye, L., Xu, H., Li, J., 2017. Analysis of major pollution factors in sea water and surface sediments and contribution of pollution sources in Xiangshan bay. Mar. Environ. Sci. 36, 328–335. https://doi.org/10.13634/j.cnki.mes.2017.03.002 (In Chinese with English abstract).
- Wu, H., Shen, J., Zhu, J., Zhang, J., Li, L., 2014. Characteristics of the Changjiang plume and its extension along the Jiangsu coast. Cont. Shelf Res. 76, 108–123. https://doi. org/10.1016/j.csr.2014.01.007.
- Wang, B., Xin, M., Wei, Q., Xie, L., 2018. A historical overview of coastal eutrophication in the China seas. Mar. Pollut. Bull. 136, 394–400. https://doi.org/10.1016/j. marpolbul.2018.09.044.
- Wu, B., Jin, H., Gao, S., Xu, J., Chen, J., 2019. Nutrient budgets and recent decadal variations in a highly eutrophic estuary: Hangzhou Bay, China. J. Coast. Res. 36 (1), 63–71. https://doi.org/10.2112/jcoastres-d-18-00071.1.
- Xu, H., Newton, A., Wolanski, E., Chen, Z., 2015. The fate of phosphorus in the Yangtze (Changjiang) estuary, China, under multi-stressors: hindsight and forecast. Estuar. Coast. Shelf Sci. 163, 1–6. https://doi.org/10.1016/j.ecss.2015.05.032.
- Xu, P., Mao, X., Jiang, W., 2016. Mapping tidal residual circulations in the outer Xiangshan Bay using a numerical model. J. Mar. Syst. 154, 181–191. https://doi. org/10.1016/j.imarsys.2015.10.002.
- Xu, J., Zhou, P., Lian, E., Wu, H., Liu, D., 2021. Spatial distribution of chlorophyll a and its relationships with environmental factors influenced by front in the Changjiang River estuary and its adjacent waters in summer 2019. Mar. Sci. Bull. 40 (5), 541–549. https://doi.org/10.11840/j.issn.1001-6392.2021.05.006 (In Chinese with English abstract).
- Yang, Z., Chen, J., Li, H., Jin, H., Gao, S., Ji, Z., Zhu, Y., Ran, L., Zhang, J., Liao, Y., Bai, Y., 2018. Sources of nitrate in Xiangshan Bay (China), as identified using nitrogen and oxygen isotopes. Estuar. Coast. Shelf Sci. 207, 109–118. https://doi. org/10.1016/j.ecss.2018.02.019.
- Yuan, Q., Li, J., Xu, L., 2014. Quantitative analysis of river morphological features in Xiangshangang Bay Basin. J. Mar. Sci. 32 (3), 50–57 (In Chinese with English abstract). https://doi.org/10.3969/j.issn.1001-909X.2014.03.007.
- Zeng, J., Pan, J., Liang, C., 2011. The Ecological Environmental Comprehensive Investigation Report in the Key Harbor of Zhejiang Province. Ocean Press, Beijing, China, pp. 39–72 (In Chinese).
- Zhang, X., Hetland, R.D., Marta-Almeida, M., DiMarco, S.F., 2012. A numerical investigation of the Mississippi and Atchafalaya freshwater transport, filling and flushing times on the Texas-Louisiana shelf. J. Geophys. Res. Oceans 117 (C11), 1–21. https://doi.org/10.1029/2012jc008108.
- Zhang, Y., Chai, F., Zhang, J., Ding, Y., Bao, M., Yan, Y., Li, H., Yu, W., Chang, L., 2022. Numerical investigation of the control factors driving Zhe-Min Coastal Current. Acta Oceanol. Sin. 41 (2), 127–138. https://doi.org/10.1007/s13131-021-1849-4.
- Zhang, J., Du, Y., Zhang, G., Chang, Y., Zhou, Y., Zhang, Z., Wu, Y., Chen, J., Zhang, A., Zhu, Z., Liu, S., 2021. Increases in the seaward river flux of nutrients driven by human migration and land-use changes in the tide-influenced delta. Sci. Total Environ. 761, 144501 https://doi.org/10.1016/j.scitotenv.2020.144501.
- Zhang, L., Jiang, X., Cai, Y., Li, Z., 2007. Comprehensive assessment of the situation of water quality at the red tide monitoring area of Xiangshan Harbor in recent four years. Transact. Oceanol. Limnol. 4, 98–103. https://doi.org/10.13984/j.cnki.cn37-1141.2007.04.020 (In Chinese with English abstract).
- Zhang, B., Wu, X., Xie, D., 2015. Variation of water and sediment in rivers to sea in recent five decades in Zhejiang Province. J. Sediment. Res. 6, 21–26. https://doi.org/10.16239/j.cnki.0468-155x.2015.06.004 (In Chinese with English abstract).
- Zheng, Y., Zhu, H., Luo, Y., 2000. Assessment on the situation of water quality at Xiangshan Port. Mar. Environ. Sci. 19 (1), 56–59 (In Chinese with English abstract).
- Zhu, B., Bai, Y., Zhang, Z., He, X., Wang, Z., Zhang, S., Dai, Q., 2022. Satellite remote sensing of water quality variation in a semi-enclosed bay (Yueqing Bay) under strong anthropogenic impact. Remote Sens. 14 (3), 1–26. https://doi.org/10.3390/ rs14030550.
- Zhu, J., Chen, C., Ding, P., Li, C., Lin, H., 2004. Does the Taiwan warm current exist in winter? Geophys. Res. Lett. 31 (12), L12302. https://doi.org/10.1029/ 2004gl019997.